We are IntechOpen,
the world's leading publisher of Open Access books
Built by scientists, for scientists

6,900
Open access books available

185,000
International authors and editors

200M
Downloads

154
Countries delivered to

Our authors are among the

TOP 1%
most cited scientists

12.2%
Contributors from top 500 universities

BOOK CITATION INDEX
CLARIVATE ANALYTICS
INDEXED

WEB OF SCIENCE™

Selection of our books indexed in the Book Citation Index
in Web of Science™ Core Collection (BKCI)

Interested in publishing with us?
Contact book.department@intechopen.com

RSTM Numerical Simulation of Channel Particulate Flow with Rough Wall

Alexander Kartushinsky, Ylo Rudi,
Medhat Hussainov, Igor Shcheglov, Sergei Tisler,
Igor Krupenski and David Stock

Additional information is available at the end of the chapter

http://dx.doi.org/10.5772/57047

1. Introduction

Turbulent gas-solid particles flows in channels have numerous engineering applications ranging from pneumatic conveying systems to coal gasifiers, chemical reactor design and are one of the most thoroughly investigated subject in the area of the particulate flows. These flows are very complex and influenced by various physical phenomena, such as particle-turbulence and particle-particle interactions, deposition, gravitational and viscous drag forces, particle rotation and lift forces etc.

The mutual effect of particles and a flow turbulence is the subject of numerous theoretical studies during several decades. These studies have reported about the influence of a gas turbulence on particles (one-way coupling) and/or particles on turbulence of a carrier gas flow (the two-way coupling) in case of high flow mass loading (the four-way coupling). The influence of particles on a gas turbulence, which consists in a turbulence attenuation or augmentation depending on the relation between the parameters of gas and particles.

There are different approaches and numerical models that describe the mutual effect of gas turbulence and particles.

The k-ε models, earlier elaborated for the turbulent particulate flows, e.g., [1-5], considered a turbulence attenuation only by the additional terms of the equations of the turbulence kinetic energy and its dissipation rate. The results obtained by these models were validated by the experimental data on the turbulent particulate free-surface flows [6].

Later on, the models [7, 8] considered both the turbulence augmentation and attenuation occurring in the pipe particulate flows depending on the flow mass loading and the Stokes

number. Then, these models have been expanded for the free-surface flows. As opposed to the k-ε models, [7, 8] considered both the turbulence augmentation caused by the velocity slip between gas and particles and the turbulence attenuation due to the change of the turbulence macroscale occurred in the particulate flow as compared to the unladen flow. The given approach has been successfully tested for various pipe and channel particulate flows.

Currently, the probability dense function (PDF) approach is widely applied for the numerical modeling of the particulate flows. The PDF models, for example, [9-13] contain more complete differential transport equations, which are written for various velocity correlations and consider both the turbulence augmentation and attenuation due to the particles.

As opposed to the pipe flows, the rectangular and square channel flows, even in case of unladen flows, are considerably anisotropic with respect to the components of the turbulence energy, that is vividly expressed near the channel walls and corners being notable as for the secondary flows. In addition, the presence of particles aggravates such anisotropy. Such flows are studied by the Reynolds stress turbulence models (RSTM), which are based on the transport equations for all components of the Reynolds stress tensor and the turbulence dissipation rate. RSTM approach allows to completely analyze the influence of particles on longitudinal, radial and azimuthal components of the turbulence kinetic energy, including also possible modifications of the cross-correlation velocity moments.

A few studies based on the RSTM approach showed its good performance and capability for simulation of the complicated flows, e.g., [14], as well for the turbulent particulate flows, for example, see [15]. Recently, the nonlinear algebraic Reynolds stress model based on the PDF approach has been proposed in [16] for the gas flow laden with small heavy particles. The original equations written for each component of Reynolds stress were reduced to their general form in terms of the turbulence energy and its dissipation rate with additional effect of the particulate phase. Eventually, the model [16] operated with the k-ε solution and did not allow to analyze the particles effect on each component of the Reynolds stress.

The 3D RSTM model, being presented in this chapter, is intended to apply for a simulation of the downward turbulent particulate flow in channel of the square cross-section (the aspect ratio of 1:6) with rough walls.

In order to approve and validate the developed model, the separate investigations have been carried out. The first study was the simulation of the downward unladen gas flow in channel of the rectangular cross-section with the smooth and rough walls. The second study relates to the downward grid-generated turbulent particulate flow in the same channel with the smooth walls.

The further stage of this study will be the development of the present model for implementa‐ tion to the particulate channel flow with the rough walls and the initial level of turbulence.

2. Governing equations and numerical method

The present 3D RSTM model is based on the two-way coupling k-L model [8] and applies the 3D RANS equations and the RSTM closure momentum equations.

The sketch of the computational flow domain is shown in Figure 1 for the case of the downward grid-generated turbulent particulate flow in the channel of square cross-section. Here u and u_s are the longitudinal components of velocities of gas and particles, respectively.
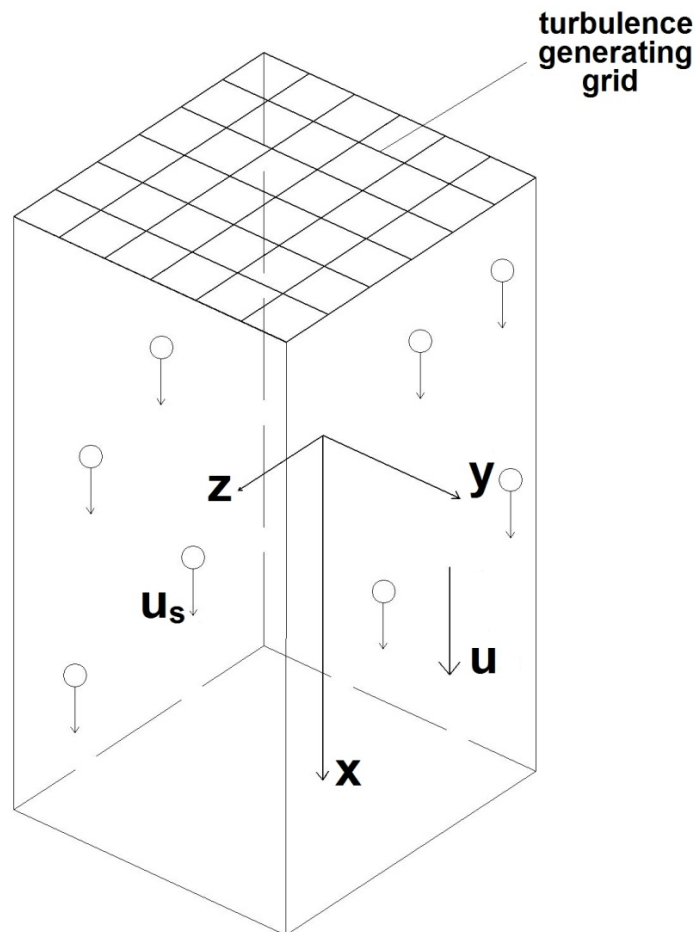
Figure 1. Downward channel grid-generated turbulent particulate flow.

2.1. Governing equations for the Reynolds stress turbulence model

The numerical simulation of the stationary incompressible 3D turbulent particulate flow in the square cross-section channel was performed by the 3D RANS model with applying of the 3D Reynolds stress turbulence model for the closure of the governing equations of gas, while the particulate phase was modeled in a frame of the 3D Euler approach with the equations closed by the two-way coupling model [8] and the eddy-viscosity concept.

The particles were brought into the developed isotropic turbulent flow set-up in channel domain, which has been preliminary computed to obtain the flow velocity field. The system of the momentum and closure equations of the gas phase are identical for the unladen while

the particle-laden flows under impact of the viscous drag force. Therefore, here is only presented the system of equations of the gas phase written for the case of the particle-laden flow in the Cartesian coordinates.

3D governing equations for the stationary gas phase of the laden flow are written together with the closure equations as follows:

continuity equation:

$$\frac{\partial u}{\partial x} + \frac{\partial v}{\partial y} + \frac{\partial w}{\partial z} = 0, \tag{1}$$

where u, v and w are the axial, transverse and spanwise time-averaged velocity components of the gas phase, respectively.

x-component of the momentum equation:

$$\frac{\partial u^2}{\partial x} + \frac{\partial uv}{\partial y} + \frac{\partial uw}{\partial z} = \frac{\partial}{\partial x}\left(2v\frac{\partial u}{\partial x} - \overline{u'^2}\right) + \frac{\partial}{\partial y}\left[v\left(\frac{\partial u}{\partial y} + \frac{\partial v}{\partial x}\right) - \overline{u'v'}\right] +$$
$$+ \frac{\partial}{\partial z}\left[v\left(\frac{\partial u}{\partial z} + \frac{\partial w}{\partial x}\right) - \overline{u'w'}\right] - \frac{\partial p}{\rho\partial x} - \alpha C_D' \frac{(u - u_s)}{\tau_p}, \tag{2}$$

y-component of the momentum equation:

$$\frac{\partial uv}{\partial x} + \frac{\partial v^2}{\partial y} + \frac{\partial vw}{\partial z} = \frac{\partial}{\partial x}\left[v\left(\frac{\partial u}{\partial y} + \frac{\partial v}{\partial x}\right) - \overline{u'v'}\right] + \frac{\partial}{\partial y}\left(2v\frac{\partial v}{\partial y} - \overline{v'^2}\right) +$$
$$+ \frac{\partial}{\partial z}\left[v\left(\frac{\partial v}{\partial z} + \frac{\partial w}{\partial y}\right) - \overline{v'w'}\right] - \frac{\partial p}{\rho\partial y} - \alpha C_D' \frac{(v - v_s)}{\tau_p}, \tag{3}$$

z-component of the momentum equation:

$$\frac{\partial uw}{\partial x} + \frac{\partial vw}{\partial y} + \frac{\partial w^2}{\partial z} = \frac{\partial}{\partial x}\left[v\left(\frac{\partial u}{\partial z} + \frac{\partial w}{\partial x}\right) - \overline{u'w'}\right] + \frac{\partial}{\partial y}\left[v\left(\frac{\partial v}{\partial z} + \frac{\partial w}{\partial y}\right) - \overline{v'w'}\right]$$
$$+ \frac{\partial}{\partial z}\left(2v\frac{\partial w}{\partial z} - \overline{w'^2}\right) - \frac{\partial p}{\rho\partial z} - \alpha C_D' \frac{(w - w_s)}{\tau_p} \tag{4}$$

the transport equation of the x-normal component of the Reynolds stress:

$$\frac{\partial\left(u\overline{u'^2}\right)}{\partial x}+\frac{\partial\left(v\overline{u'^2}\right)}{\partial y}+\frac{\partial\left(w\overline{u'^2}\right)}{\partial z}=\frac{\partial}{\partial x}\left[\left(C_sT\overline{u'^2}+\nu\right)\frac{\partial\overline{u'^2}}{\partial x}+C_sT\left(\overline{u'v'}\frac{\partial\overline{u'^2}}{\partial y}+\overline{u'w'}\frac{\partial\overline{u'^2}}{\partial z}\right)\right]$$

$$+\frac{\partial}{\partial y}\left[\left(C_sT\overline{v'^2}+\nu\right)\frac{\partial\overline{u'^2}}{\partial y}+C_sT\left(\overline{u'v'}\frac{\partial\overline{u'^2}}{\partial x}+\overline{v'w'}\frac{\partial\overline{u'^2}}{\partial z}\right)\right]$$

$$\frac{\partial}{\partial z}\left[\left(C_sT\overline{w'^2}+\nu\right)\frac{\partial\overline{u'^2}}{\partial z}+C_sT\left(\overline{u'w'}\frac{\partial\overline{u'^2}}{\partial x}+\overline{v'w'}\frac{\partial\overline{u'^2}}{\partial y}\right)\right]+P_{uu}+R_{uu}+\alpha C'_D\frac{\left(u-u_s\right)^2}{\tau_p}-\varepsilon_h \qquad (5)$$

the transport equation of the y-normal component of the Reynolds stress:

$$\frac{\partial\left(u\overline{v'^2}\right)}{\partial x}+\frac{\partial\left(v\overline{v'^2}\right)}{\partial y}+\frac{\partial\left(w\overline{v'^2}\right)}{\partial z}=\frac{\partial}{\partial x}\left[\left(C_sT\overline{u'^2}+\nu\right)\frac{\partial\overline{v'^2}}{\partial x}+C_sT\left(\overline{u'v'}\frac{\partial\overline{v'^2}}{\partial y}+\overline{u'w'}\frac{\partial\overline{v'^2}}{\partial z}\right)\right]$$

$$+\frac{\partial}{\partial y}\left[\left(C_sT\overline{v'^2}+\nu\right)\frac{\partial\overline{v'^2}}{\partial y}+C_sT\left(\overline{u'v'}\frac{\partial\overline{v'^2}}{\partial x}+\overline{v'w'}\frac{\partial\overline{v'^2}}{\partial z}\right)\right]+$$

$$+\frac{\partial}{\partial z}\left[\left(C_sT\overline{w'^2}+\nu\right)\frac{\partial\overline{v'^2}}{\partial z}+C_sT\left(\overline{u'w'}\frac{\partial\overline{v'^2}}{\partial x}+\overline{v'w'}\frac{\partial\overline{v'^2}}{\partial y}\right)\right] \qquad (6)$$

$$+P_{vv}+R_{vv}+\alpha C'_D\frac{\left(v-v_s\right)^2}{\tau_p}-\varepsilon_h$$

the transport equation of the z-normal component of the Reynolds stress:

$$\frac{\partial\left(u\overline{w'^2}\right)}{\partial x}+\frac{\partial\left(v\overline{w'^2}\right)}{\partial y}+\frac{\partial\left(w\overline{w'^2}\right)}{\partial z}=\frac{\partial}{\partial x}\left[\left(C_sT\overline{u'^2}+\nu\right)\frac{\partial\overline{w'^2}}{\partial x}+C_sT\left(\overline{u'v'}\frac{\partial\overline{w'^2}}{\partial y}+\overline{u'w'}\frac{\partial\overline{w^2}}{\partial z}\right)\right]$$

$$+\frac{\partial}{\partial y}\left[\left(C_sT\overline{v'^2}+\nu\right)\frac{\partial\overline{w'^2}}{\partial y}+C_sT\left(\overline{u'v'}\frac{\partial\overline{w'^2}}{\partial x}+\overline{v'w'}\frac{\partial\overline{w'^2}}{\partial z}\right)\right] \qquad (7)$$

$$+\frac{\partial}{\partial z}\left[\left(C_sT\overline{w'^2}+\nu\right)\frac{\partial\overline{w'^2}}{\partial z}+C_sT\left(\overline{u'w'}\frac{\partial\overline{w'^2}}{\partial x}+\overline{v'w'}\frac{\partial\overline{w'^2}}{\partial y}\right)\right]+P_{ww}+R_{ww}+\alpha C'_D\frac{\left(w-w_s\right)^2}{\tau_p}-\varepsilon_h$$

the transport equation of the xy shear stress component of the Reynolds stress:

$$\frac{\partial\left(u\overline{u'v'}\right)}{\partial x} + \frac{\partial\left(v\overline{u'v'}\right)}{\partial y} + \frac{\partial\left(w\overline{u'v'}\right)}{\partial z} =$$

$$= \frac{\partial}{\partial x}\left[\left(C_sT\overline{u'^2}+\nu\right)\frac{\partial\overline{u'v'}}{\partial x} + C_sT\left(\overline{u'v'}\frac{\partial\overline{u'v'}}{\partial y}+\overline{u'w'}\frac{\partial\overline{u'v'}}{\partial z}\right)\right] + \frac{\partial}{\partial y}\left[\left(C_sT\overline{v'^2}+\nu\right)\frac{\partial\overline{u'v'}}{\partial y}\right.$$

$$+C_sT\left(\overline{u'v'}\frac{\partial\overline{u'v'}}{\partial x}+\overline{v'w'}\frac{\partial\overline{u'v'}}{\partial z}\right)\right] + \frac{\partial}{\partial z}\left[\left(C_sT\overline{w'^2}+\nu\right)\frac{\partial\overline{u'v'}}{\partial z} + C_sT\left(\overline{u'w'}\frac{\partial\overline{u'v'}}{\partial x}+\overline{v'w'}\frac{\partial\overline{u'v'}}{\partial y}\right)\right]+$$

$$+P_{uv}+R_{uv}$$

(8)

the transport equation of the xz shear stress component of the Reynolds stress:

$$\frac{\partial\left(u\overline{u'w'}\right)}{\partial x} + \frac{\partial\left(v\overline{u'w'}\right)}{\partial y} + \frac{\partial\left(w\overline{u'w'}\right)}{\partial z} = \frac{\partial}{\partial x}\left[\left(C_sT\overline{u'^2}+\nu\right)\frac{\partial\overline{u'w'}}{\partial x} + C_sT\left(\overline{u'v'}\frac{\partial\overline{u'w'}}{\partial y}+\overline{u'w'}\frac{\partial\overline{u'w'}}{\partial z}\right)\right]$$

$$+\frac{\partial}{\partial y}\left[\left(C_sT\overline{v'^2}+\nu\right)\frac{\partial\overline{u'w'}}{\partial y}+C_sT\left(\overline{u'v'}\frac{\partial\overline{u'w'}}{\partial x}+\overline{v'w'}\frac{\partial\overline{u'w'}}{\partial z}\right)\right]$$

$$+\frac{\partial}{\partial z}\left[\left(C_sT\overline{w'^2}+\nu\right)\frac{\partial\overline{u'w'}}{\partial z}+C_sT\left(\overline{u'w'}\frac{\partial\overline{u'w'}}{\partial x}+\overline{v'w'}\frac{\partial\overline{u'w'}}{\partial y}\right)\right] + P_{uw}+R_{uw}$$

(9)

the transport equation of the yz shear stress component of the Reynolds stress:

$$\frac{\partial\left(u\overline{v'w'}\right)}{\partial x} + \frac{\partial\left(v\overline{v'w'}\right)}{\partial y} + \frac{\partial\left(w\overline{v'w'}\right)}{\partial z}$$

$$= \frac{\partial}{\partial x}\left[\left(C_sT\overline{u'^2}+\nu\right)\frac{\partial\overline{v'w'}}{\partial x} + C_sT\left(\overline{u'v'}\frac{\partial\overline{v'w'}}{\partial y}+\overline{u'w'}\frac{\partial\overline{v'w'}}{\partial z}\right)\right] + \frac{\partial}{\partial y}\left[\left(C_sT\overline{v'^2}+\nu\right)\frac{\partial\overline{v'w'}}{\partial y}\right.$$

$$+C_sT\left(\overline{u'v'}\frac{\partial\overline{v'w'}}{\partial x}+\overline{v'w'}\frac{\partial\overline{v'w'}}{\partial z}\right)\right] + \frac{\partial}{\partial z}\left[\left(C_sT\overline{w'^2}+\nu\right)\frac{\partial\overline{v'w'}}{\partial z} + C_sT\left(\overline{u'w'}\frac{\partial\overline{v'w'}}{\partial x}+\overline{v'w'}\frac{\partial\overline{v'w'}}{\partial y}\right)\right]$$

$$+P_{vw}+R_{vw}$$

(10)

the transport equation of the dissipation rate of the turbulence kinetic energy:

$$\frac{\partial u_0 \varepsilon_0}{\partial x} + \frac{\partial v_0 \varepsilon_0}{\partial y} + \frac{\partial w_0 \varepsilon_0}{\partial z} = \frac{\partial}{\partial x}\left[\left(C_\varepsilon T_0 \overline{u_0'^2} + \nu\right)\frac{\partial \varepsilon_0}{\partial x} + C_\varepsilon T_0\left(\overline{u_0'v_0'}\frac{\partial \varepsilon_0}{\partial y} + \overline{u_0'w_0'}\frac{\partial \varepsilon_0}{\partial z}\right)\right]$$

$$+\frac{\partial}{\partial y}\left[\left(C_\varepsilon T_0 \overline{v_0'^2} + \nu\right)\frac{\partial \varepsilon_0}{\partial y} + C_\varepsilon T_0\left(\overline{u_0'v_0'}\frac{\partial \varepsilon_0}{\partial x} + \overline{v_0'w_0'}\frac{\partial \varepsilon_0}{\partial z}\right)\right] + \frac{\partial}{\partial z}\left[\left(C_\varepsilon T_0 \overline{w_0'^2} + \nu\right)\frac{\partial \varepsilon_0}{\partial z}\right] \quad (11)$$

$$+C_\varepsilon T_0\left(\overline{u_0'w_0'}\frac{\partial \varepsilon_0}{\partial x} + \overline{v_0'w_0'}\frac{\partial \varepsilon_0}{\partial y}\right)\right] + C_{\varepsilon 1}\frac{P\varepsilon_0}{k_0} - C_{\varepsilon 2}\frac{\varepsilon_0^2}{k_0}$$

The given system of the transport equations (Eqs. 1 – 11) is based on the model [17] with applying of the numerical constants taken from [18]: C_R=1.8, C_2=0.6, C_s=0.22, C_ε=0.18, $C_{\varepsilon 1}$=1.44, $C_{\varepsilon 2}$=1.92. Here $T_0 = \frac{k_0}{\varepsilon_0}$ and $T = \frac{k}{\varepsilon}$ are the turbulence integral time scales for the unladen and particle-laden flows, respectively. $k=0.5(\overline{u'^2}+\overline{v'^2}+\overline{w'^2})$ and $k_0=0.5(\overline{u_0'^2}+\overline{v_0'^2}+\overline{w_0'^2})$ are the turbulence kinetic energy of gas in the particle-laden and in the unladen flows, respectively; ε and ε_0 are the dissipation rates of the turbulence kinetic energy in the particle-laden and unladen flows, respectively; τ_p is the Stokesian particle response time, $\tau_p = \frac{\rho_p \delta^2}{18\rho\nu}$; ν is the gas viscosity; $(u-u_s)$, $(v-v_s)$ and $(w-w_s)$ are the components of the slip velocity.

The additional terms of Eqs. (2 – 7) pertain to presence of particles in the flow and contain the particle mass concentration α. The influence of particles on gas is considered by the aerodynamic drag force in the momentum equations (the last term of the right-hand sides of Eqs. 2 – 4), and by the turbulence generation and attenuation effects contained in the transport equations of components of the Reynolds stress (the penultimate and last terms of the right-hand sides of Eqs. (5 – 7), respectively). The given model applies the two-way coupling approach [8], where the turbulence generation terms are proportional to the squared slip velocity, and the turbulence attenuation terms are expressed via the hybrid length scale L_h and the hybrid dissipation rate ε_h of the particle-laden flow, where L_h is calculated as the harmonic average of the integral length scale of the unladen flow L_0 and the interparticle distance λ. Here $\lambda = \delta(\sqrt[3]{\pi\rho_p/6\rho\alpha}-1)$, $L_0 = \frac{k_0^{3/2}}{\varepsilon_0}$, $L_h = \frac{2L_0\lambda}{L_0+\lambda}$, $\varepsilon_h = \frac{k^{3/2}}{L_h}$. The particles influence on the shear Reynolds stress components is considered in Eqs. (8 – 10) indirectly via the averaged velocity flow field (u, v, w).

The production terms P are determined according to [18] as follows:

$$P_{uu} = -2\left(\overline{u'^2}\frac{\partial u}{\partial x} + \overline{u'v'}\frac{\partial u}{\partial y} + \overline{u'w'}\frac{\partial u}{\partial z}\right), \quad (12)$$

$$P_{vv} = -2\left(\overline{u'v'}\frac{\partial v}{\partial x} + \overline{v'^2}\frac{\partial v}{\partial y} + \overline{v'w'}\frac{\partial v}{\partial z} \right), \tag{13}$$

$$P_{ww} = -2\left(\overline{u'w'}\frac{\partial w}{\partial x} + \overline{v'w'}\frac{\partial w}{\partial y} + \overline{w'^2}\frac{\partial w}{\partial z} \right), \tag{14}$$

$$P_{uv} = -\left(\overline{u'^2}\frac{\partial v}{\partial x} + \overline{u'v'}\frac{\partial v}{\partial y} + \overline{u'w'}\frac{\partial v}{\partial z} + \overline{u'v'}\frac{\partial u}{\partial x} + \overline{v'^2}\frac{\partial u}{\partial y} + \overline{v'w'}\frac{\partial u}{\partial z} \right), \tag{15}$$

$$P_{uw} = -\left(\overline{u'^2}\frac{\partial w}{\partial x} + \overline{u'v'}\frac{\partial w}{\partial y} + \overline{u'w'}\frac{\partial w}{\partial z} + \overline{u'w'}\frac{\partial u}{\partial x} + \overline{v'w'}\frac{\partial u}{\partial y} + \overline{w'^2}\frac{\partial u}{\partial z} \right), \tag{16}$$

$$P_{vw} = -\left(\overline{u'v'}\frac{\partial w}{\partial x} + \overline{v'^2}\frac{\partial w}{\partial y} + \overline{v'w'}\frac{\partial w}{\partial z} + \overline{u'w'}\frac{\partial v}{\partial x} + \overline{v'w'}\frac{\partial v}{\partial y} + \overline{w'^2}\frac{\partial v}{\partial z} \right), \tag{17}$$

$$P = \frac{1}{2}\left(P_{uu} + P_{vv} + P_{ww} \right) = \overline{u'^2}\frac{\partial u}{\partial x} + \overline{u'v'}\frac{\partial u}{\partial y} + \overline{u'w'}\frac{\partial u}{\partial z} + \overline{u'v'}\frac{\partial v}{\partial x} + \overline{v'^2}\frac{\partial v}{\partial y} + \overline{v'w'}\frac{\partial v}{\partial z}$$
$$+ \overline{u'w'}\frac{\partial w}{\partial x} + \overline{v'w'}\frac{\partial w}{\partial y} + \overline{w'^2}\frac{\partial w}{\partial z} \tag{18}$$

The diffusive or second order partial differentiation over Cartesian coordinates, i.e. the first three terms in Eqs. (5 – 11) are given, e.g. in [18]. The anisotropy terms R of the normal and shear components of the Reynolds stress $\overline{u'^2}$, $\overline{v'^2}$, $\overline{w'^2}$, $\overline{u'v'}$, $\overline{u'w'}$, $\overline{v'w'}$, are defined by various pressure-rate-of-strain models of the isotropic turbulence written in terms of variation of constants C_R and C_2 [18] as follows:

$$R_{uu} = -\frac{(C_R - 1)}{T}\left(\overline{u'^2} - \frac{2}{3}k \right) - C_2\left(P_{uu} - \frac{2}{3}P \right), \tag{19}$$

$$R_{vv} = -\frac{(C_R - 1)}{T}\left(\overline{v'^2} - \frac{2}{3}k \right) - C_2\left(P_{vv} - \frac{2}{3}P \right), \tag{20}$$

$$R_{ww} = -\frac{(C_R - 1)}{T}\left(\overline{w'^2} - \frac{2}{3}k \right) - C_2\left(P_{ww} - \frac{2}{3}P \right), \tag{21}$$

$$R_{uv} = -\frac{(C_R - 1)\overline{u'v'}}{T} - C_2 P_{uv}, \tag{22}$$

$$R_{uw} = -\frac{(C_R - 1)\overline{u'w'}}{T} - C_2 P_{uw}, \tag{23}$$

$$R_{vw} = -\frac{(C_R - 1)\overline{v'w'}}{T} - C_2 P_{vw}. \tag{24}$$

The relative friction coefficient C'_D is expressed as $C'_D = 1 + 0.15 \text{Re}_s^{0.687}$ for the non-Stokesian streamlining of particle. The particle Reynolds number Re_s is calculated according to [19] as $\text{Re}_s = \delta \sqrt{(u - u_s)^2 + (v - v_s)^2 + (w - w_s)^2} / v$.

3D governing equations for the particulate phase are written as follows:

the particle mass conservation equation:

$$\frac{\partial(\alpha u_s)}{\partial x} + \frac{\partial(\alpha v_s)}{\partial y} + \frac{\partial(\alpha w_s)}{\partial z} = \frac{\partial}{\partial x} D_s \frac{\partial \alpha}{\partial x} + \frac{\partial}{\partial y} D_s \frac{\partial \alpha}{\partial y} + \frac{\partial}{\partial z} D_s \frac{\partial \alpha}{\partial z}, \tag{25}$$

x-component of the momentum equation:

$$\frac{\partial(\alpha u_s v_s)}{\partial x} + \frac{\partial(\alpha v_s^2)}{\partial y} + \frac{\partial(\alpha v_s w_s)}{\partial z} = \frac{\partial}{\partial x}\left[\alpha v_s \left(\frac{\partial u_s}{\partial y} + \frac{\partial v_s}{\partial x}\right)\right] + \frac{\partial}{\partial y}\alpha\left(2 v_s \frac{\partial v_s}{\partial y} - \frac{2}{3} k_s\right)$$
$$+ \frac{\partial}{\partial z}\left[\alpha v_s \left(\frac{\partial v_s}{\partial z} + \frac{\partial w_s}{\partial y}\right)\right] + \alpha C'_D \frac{(v - v_s)}{\tau_p} - \alpha g \left(1 - \frac{\rho}{\rho_p}\right) \tag{26}$$

y-component of the momentum equation:

$$\frac{\partial(\alpha u_s v_s)}{\partial x} + \frac{\partial(\alpha v_s^2)}{\partial y} + \frac{\partial(\alpha v_s w_s)}{\partial z} = \frac{\partial}{\partial x}\left[\alpha v_s \left(\frac{\partial u_s}{\partial y} + \frac{\partial v_s}{\partial x}\right)\right] + \frac{\partial}{\partial y}\varepsilon\left(2 v_s \frac{\partial v_s}{\partial y} - \frac{2}{3} k_s\right)$$
$$+ \frac{\partial}{\partial z}\left[\alpha v_s \left(\frac{\partial v_s}{\partial z} + \frac{\partial w_s}{\partial y}\right)\right] + \alpha C'_D \frac{(v - v_s)}{\tau_p}, \tag{27}$$

z-component of the momentum equation:

$$\frac{\partial(\alpha u_s w_s)}{\partial x} + \frac{\partial(\alpha v_s w_s)}{\partial y} + \frac{\partial(\alpha w_s^2)}{\partial z} = \frac{\partial}{\partial x}\left[\alpha v_s\left(\frac{\partial u_s}{\partial z} + \frac{\partial w_s}{\partial x}\right)\right] + \frac{\partial}{\partial y}\left[\alpha v_s\left(\frac{\partial v_s}{\partial z} + \frac{\partial w_s}{\partial y}\right)\right]$$
$$+\frac{\partial}{\partial z}\alpha\left(2v_s\frac{\partial w_s}{\partial z} - \frac{2}{3}k_s\right) + \alpha C_D'\frac{(w - w_s)}{\tau_p}.$$

(28)

The closure model for the transport equations of the particulate phase was applied to the PDF model [20], where the turbulent kinetic energy of dispersed phase, the coefficients of the turbulent viscosity and turbulent diffusion of the particulate phase are determined as follows, respectively:

$$k_s = \left[1 - \exp\left(-\frac{T_0}{\tau_p'}\right)\right]k, \quad v_s = \left(v_t + \frac{\tau_p'k}{3}\right)\left[1 - \exp\left(-\frac{T_0}{\tau_p'}\right)\right], \quad D_s = \frac{2k}{3}\left(1 + \frac{T_0}{\tau}\right)\left[1 - \exp\left(-\frac{T_0}{\tau}\right)\right],$$
$$v_s = \left(v_t + \frac{\tau_p'k}{3}\right)\left[1 - \exp\left(-\frac{T_0}{\tau_p'}\right)\right],$$

(29)

where v_t is the turbulent viscosity, $v_t = 0.09\dfrac{k_0^2}{\varepsilon_0}$ and $\tau_p' = \tau_p / C_D'$ is the particle response time with respect of correction of the particles motion to the non-Stokesian regime.

2.2. Boundary conditions for the Reynolds stress turbulence model

The grid-generated turbulent flow is vertical, and it is symmetrical with respect to the vertical axis for both y-and z-directions. Therefore, the symmetry conditions are set at the flow axis, and the wall conditions are set at the wall. In case of the rough and smooth walls the flow was asymmetrical over the y-direction and symmetrical over the z-direction.

The axisymmetric conditions are written as follows:

for $z = 0$:

$$\frac{\partial u}{\partial z} = \frac{\partial \overline{u'^2}}{\partial z} = \frac{\partial \overline{v'^2}}{\partial z} = \frac{\partial \overline{w'^2}}{\partial z} = \frac{\partial \varepsilon}{\partial z} = \frac{\partial u_s}{\partial z} = \frac{\partial \alpha}{\partial z} = v = w = \overline{u'v'} = \overline{u'w'} = \overline{v'w'} = v_s = w_s = 0;$$

(30)

for $z = 0.5h$:

$$u^+ = \frac{u}{v_*} = \begin{cases} z^+ \\ \dfrac{1}{\text{æ}}\ln z^+ + B_1 \end{cases}.$$

(31)

The wall conditions are written as follows:

for $y = 0.5h$ (smooth wall):

$$u^+ = \frac{u}{v_*} = \begin{cases} y^+ \\ \frac{1}{\text{æ}} \ln y^+ + B_1 \end{cases}, \tag{32}$$

for $y = -0.5h$ (rough wall):

$$u^+ = \frac{u}{v_*} = \frac{1}{\text{æ}} \ln \frac{4 \Delta y}{s} + B_2 \, ; \, v = w = 0 \tag{33}$$

where h is the channel width; v_* is the friction velocity of gas; æ is von Karman's constant, æ =0.41; the wall coordinates y^+ and z^+ correspond to the transverse and spanwise directions, respectively; s is a roughness height. The friction velocity of gas v_* is determined according to [21] as $v_* = (c_\mu / 2)^{0.25} \sqrt{k}$, where c_μ is the numerical constant of the k-ε model, c_μ=0.09; B_1=5.2 for the smooth wall and B_2=8.5 for the rough wall; Δy is the grid step of the control volume.

For the normal and shear stresses and dissipation rate of the unladen flow calculated at the wall, the boundary conditions are set based on the "wall-function" according to [18] with the following relationships for the production and dissipation terms:

for $y = 0.5h$:

$$P_{uu} = -\overline{u'v'} \frac{\partial u}{\partial y}, \, P_{vv} = P_{ww} = P_{uv} = P_{uw} = P_{vw} = 0, \tag{34}$$

$$\varepsilon = \frac{2 c_\mu^{0.75} k^{1.5}}{\text{æ} \Delta y}, \tag{35}$$

for $z = 0.5h$:

$$P_{uu} = -\overline{u'w'} \frac{\partial u}{\partial z}, \, P_{vv} = P_{ww} = P_{uv} = P_{uw} = P_{vw} = 0, \tag{36}$$

$$\varepsilon = \frac{2 c_\mu^{0.75} k^{1.5}}{\text{æ} \Delta z}. \tag{37}$$

The boundary conditions for the particulate phase are set at the wall as follows:

for $y = 0.5h$:

$$\frac{\partial u_s}{\partial y} = -\lambda u_s, \quad \frac{\partial w_s}{\partial y} = -\lambda w_s, \quad \frac{\partial \alpha}{\partial y} = D_s \alpha, \quad v_s = 0, \tag{38}$$

for $z = 0.5h$:

$$\frac{\partial u_s}{\partial z} = -\lambda u_s; \quad \frac{\partial v_s}{\partial z} = -\lambda v_s, \quad \frac{\partial \alpha}{\partial z} = D_s \alpha \quad w_s = 0; \tag{39}$$

At the exit of the channel the following boundary conditions are set:

$$\frac{\partial u}{\partial x} = \frac{\partial v}{\partial x} = \frac{\partial w}{\partial x} = \frac{\partial \overline{u'^2}}{\partial x} = \frac{\partial \overline{v'^2}}{\partial x} = \frac{\partial \overline{w'^2}}{\partial x} = \frac{\partial \overline{u'v'}}{\partial x} =$$
$$= \frac{\partial \overline{u'w'}}{\partial x} = \frac{\partial \overline{v'w'}}{\partial x} = \frac{\partial \varepsilon}{\partial x} = \frac{\partial u_s}{\partial x} = \frac{\partial v_s}{\partial x} = \frac{\partial w_s}{\partial x} = \frac{\partial \alpha}{\partial x} = 0. \tag{40}$$

Additionally, the initial boundary conditions are set for three specific cases:

1. the low level of the initial intensity of turbulence that usually occurs at the axis of the channel turbulent flow;

2. the high level of the initial turbulence generated by two different grids:

a. small grid of the mesh size M=4.8 mm;

b. large grid with mesh size of M=10 mm.

2.3. Numerical method

The control volume method was applied to solve the 3D partial differential equations written for the unladen flow (Eqs. 1 – 11) and the particulate phase (Eqs. 26 – 29), respectively, with taking into account the boundary conditions (Eqs. 30 – 40). The governing equations were solved using the implicit lower and upper (ILU) matrix decomposition method with the flux-blending differed-correction and upwind-differencing schemes [21]. This method is utilized for the calculations of the particulate turbulent flows in channels of the rectangular and square cross-sections. The calculations were performed in the dimensional form for all the flow conditions. The number of the control volumes was 1120000.

3. Numerical results

The validation of the present model took place in two stages.

In case of the unladen flow, the model was validated by comparison of the kinetic (normal) components of stresses with the experimental data [22] obtained for the specially constructed horizontal turbulent gas flow in the channel of rectangular cross-section (the aspect ratio of 1:6) of 54 mm width with the smooth and rough walls for the flow Reynolds number Re=56000 and the roughness height of 3.18 mm.
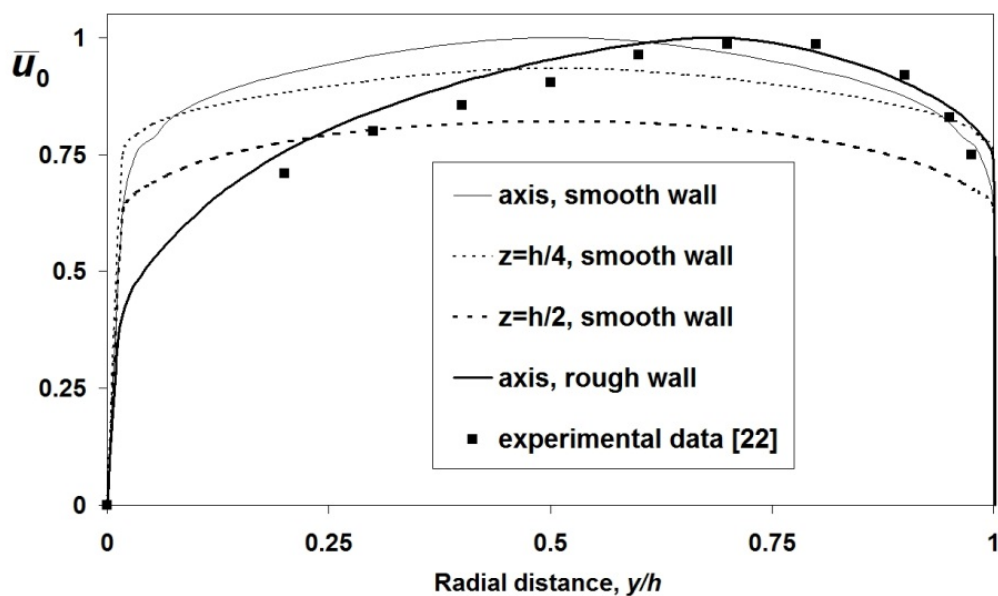
Figure 2. Numerical and experimental [22] distributions of the longitudinal component of the averaged velocity of gas over the channel cross-section.

Figure 2 shows the distributions of the longitudinal component of the averaged velocity of gas u_0 over the channel cross-section for two cases: i) the smooth walls and ii) the left wall is rough and the right wall is smooth for the mean flow velocity 15.5 m/s. Figure 3 shows the distributions of the normalized Reynolds normal stress tensor components obtained for the same conditions as Figure 2. The radial distance y/h=0 corresponds to the rough wall and y/h=1 corresponds to the smooth wall. The subscript "0" denotes the unladen flow conditions.

One can see that in case of the smooth channel walls, the mean flow velocity and the components of the turbulence kinetic energy demonstrate the representative symmetrical turbulent distributions over the cross-section of the rectangular channel. The transfer to the rough walls results in transformation of the given distributions. The maximum of the distribution of the time-averaged flow velocity moves towards the smooth wall. The similar change relates to the distributions of each component of the turbulence kinetic energy. These numerical results demonstrates the satisfactory agreement with the experimental data [22].
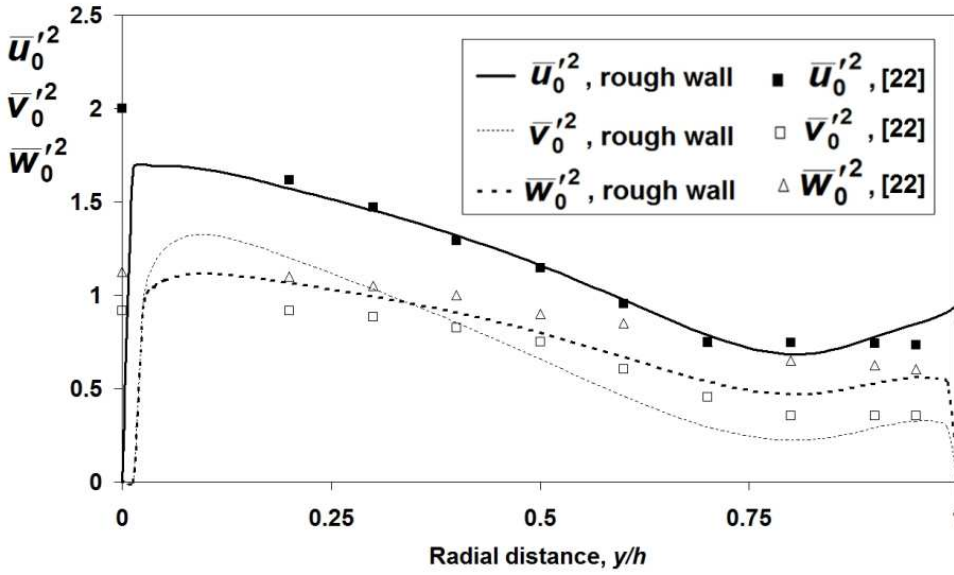
Figure 3. Numerical and experimental [22] distributions of the normalized Reynolds normal stress tensor components.

The next step of the study was the extension of the present model to the gas-solid particles grid-generated turbulent downward vertical channel flow. The experimental data [23] obtained for the channel flow of 200 mm square cross-section loaded with 700-μm glass beads of the physical density 2500 kg/m^3 was used for the model validation. The mean flow velocity was 9.5 m/s, the flow mass loading was 0.14 kg dust/kg air. The grids of the square mesh size M=4.8 and 10 mm were used for generating of the flow initial turbulence length scale.

The validity criterion was based on the satisfactory agreement of the axial turbulence decay curves occurring behind different grids in the unladen and particle-laden flows obtained by the given RSTM model and by the experiments [23]. Figure 4 demonstrates such agreement for the grid M=4.8 mm.

Figure 5 shows the decay curves calculated by the present RSTM model for the grids M=4.8 and 10 mm. As follows from Figs. 4 and 5, the pronounced turbulence enhancement by particles is observed for both grids. The character of the turbulence attenuation occurring along the flow axis agrees with the behavior of the decay curves in the grid-generated turbulent flows described in [24].

Figures 6 – 11 show the cross-section modifications of three components of the Reynolds stress, Δ_u, Δ_v, Δ_w, caused by 700-μm glass beads, calculated by the presented RSTM model at two locations of the initial period of the grid-generated turbulence decay x/M =46 and 93 as well as beyond it for $x/M \approx 200$. Here:

$$\Delta_u = \frac{\overline{u'^2} - \overline{u_0'^2}}{\overline{u_0'^2}}, \%, \quad \Delta_v = \frac{\overline{v'^2} - \overline{v_0'^2}}{\overline{v_0'^2}} \%, \quad \Delta_w = \frac{\overline{w'^2} - \overline{w_0'^2}}{\overline{w_0'^2}} \%. \quad (41)$$
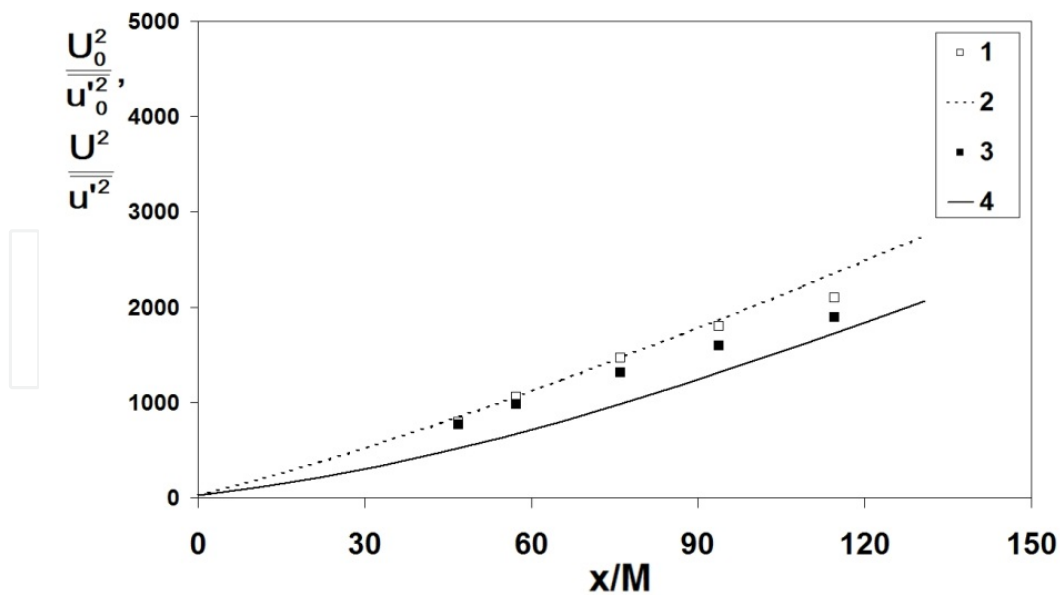
Figure 4. Axial turbulence decay behind the grid M=4.8 mm: 1 and 3 are the data [23] got for the unladen and parti-cle-laden flows, respectively; 2 and 4 are the numerical data obtained for the same conditions.
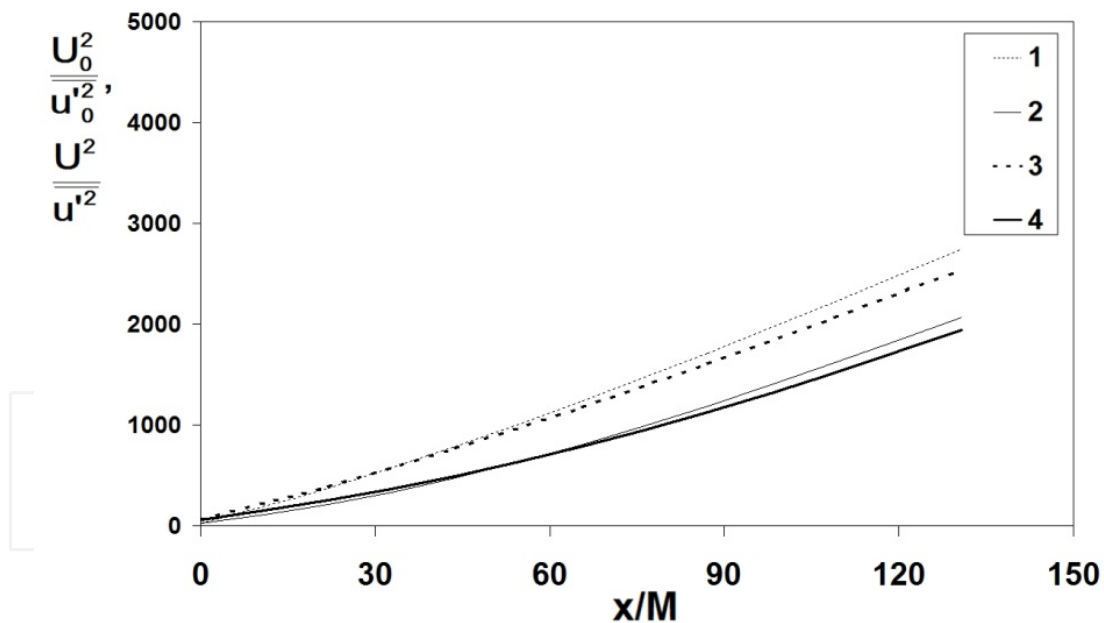

Figure 5. The calculated axial turbulence decay behind the grids: 1 and 2 are the data got for the unladen and parti-cle-laden flow, respectively, at M=4.8 mm, 3 and 4 are the data obtained for the same conditions at M=10 mm.

One can see that the turbulence enhancement occupies over 75% of the half-width of the channel, that takes place at the initial period of the turbulence decay of the particle-laden flow as compared to the unladen flow. Along with, the distributions of Δ_u, Δ_v and Δ_w are uniform that corresponds to the initial grid-generated homogeneous isotropic turbulence, which

decays downstream (s. Figures 4 and 5). The distributions of modification of $\varDelta_u$, $\varDelta_v$ and $\varDelta_w$ remain uniform downstream. At the same time, the cross-section extent of uniformity of distributions of components of the Reynolds stress and the degree of the particles effect on turbulence decrease, since the turbulence level decreases downstream (cf. data presented for x/M =46 and 93 in Figures 6 – 11).
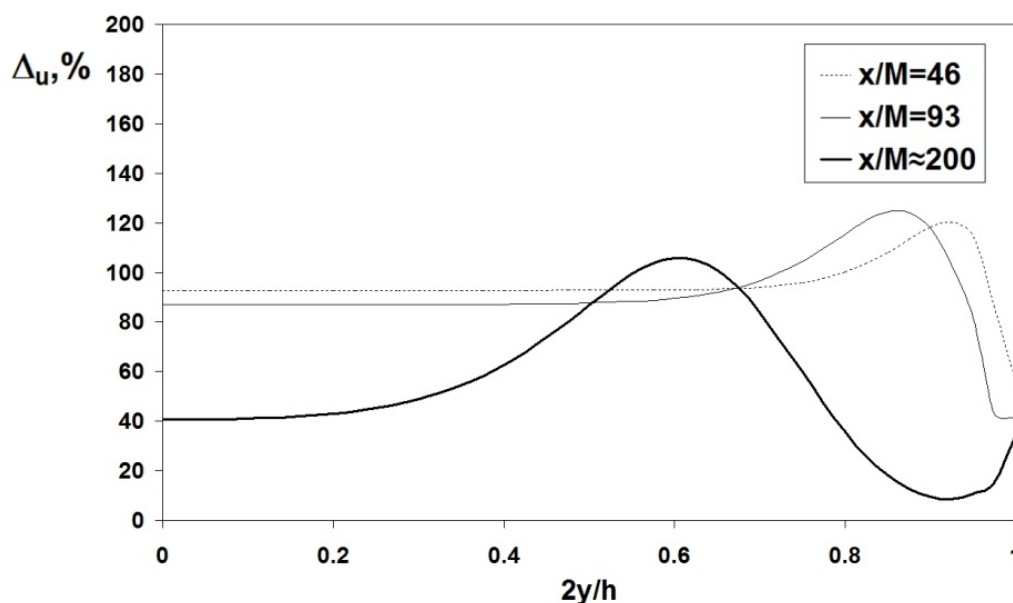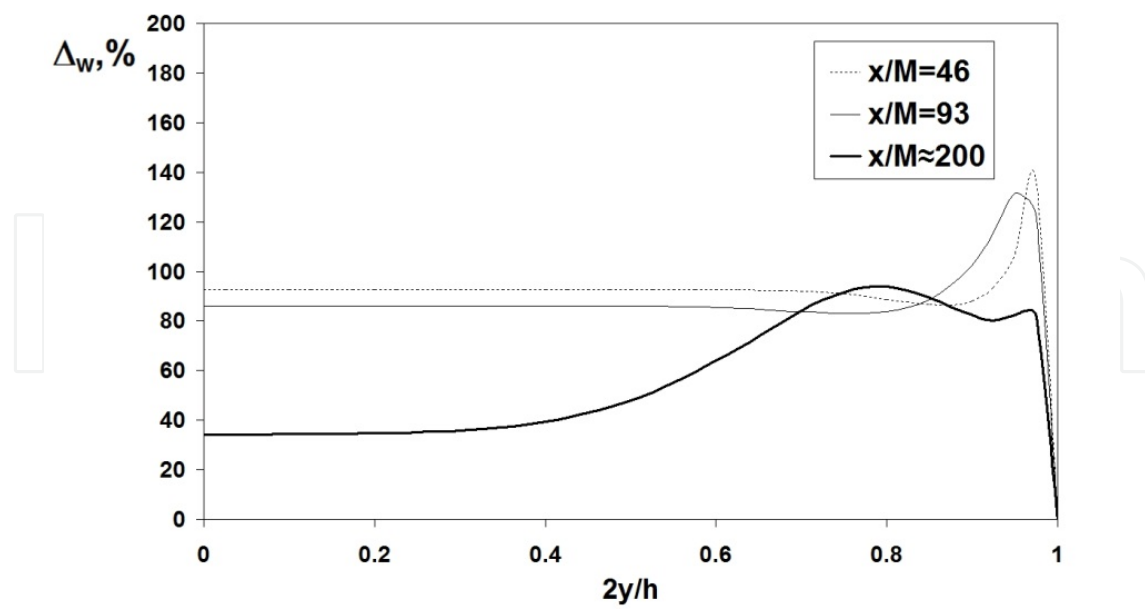

Figure 6. Effect of particles on the modification of the *x*-normal component of the Reynolds stress: *M*=4.8 mm, *z*=0.

The distributions of modification of $\varDelta_u$, $\varDelta_v$ and $\varDelta_w$ taken place beyond the initial period of the turbulence decay (location $x/M \approx 200$ at Figures 6 – 11) are typical of the channel turbulent particulate flow. One can see that in this case the turbulence enhancement becomes slower, since here the turbulence level is substantially smaller as compared with the initial period of decay, i.e. for x/M <100 (s. Figures 4 and 5). This means that the grid-generated turbulence of the particulate flow decays downstream, and this causes the decrease of the rate of turbulence enhancement due to the particles occurred beyond the initial period of the turbulence decay. As a result, the turbulence is attenuated, that is expressed in terms of decrease of $\varDelta_u$ towards the pipe wall (s. Figure 9). Such tendency has been shown qualitatively in [25].

The certain increase of $\varDelta_u$, $\varDelta_v$ and $\varDelta_w$, that is observed verge towards the wall (s. Figures 6 – 11), arises from the growth of the slip velocity (s. curves 1, 2, 3 in Figure 12). The decrease of $\varDelta_u$, $\varDelta_v$ and $\varDelta_w$ taken place in the immediate vicinity of the wall is caused by the decrease of the length scale of the energy-containing vortices and, thus, the increase of the dissipation of the turbulence kinetic energy.
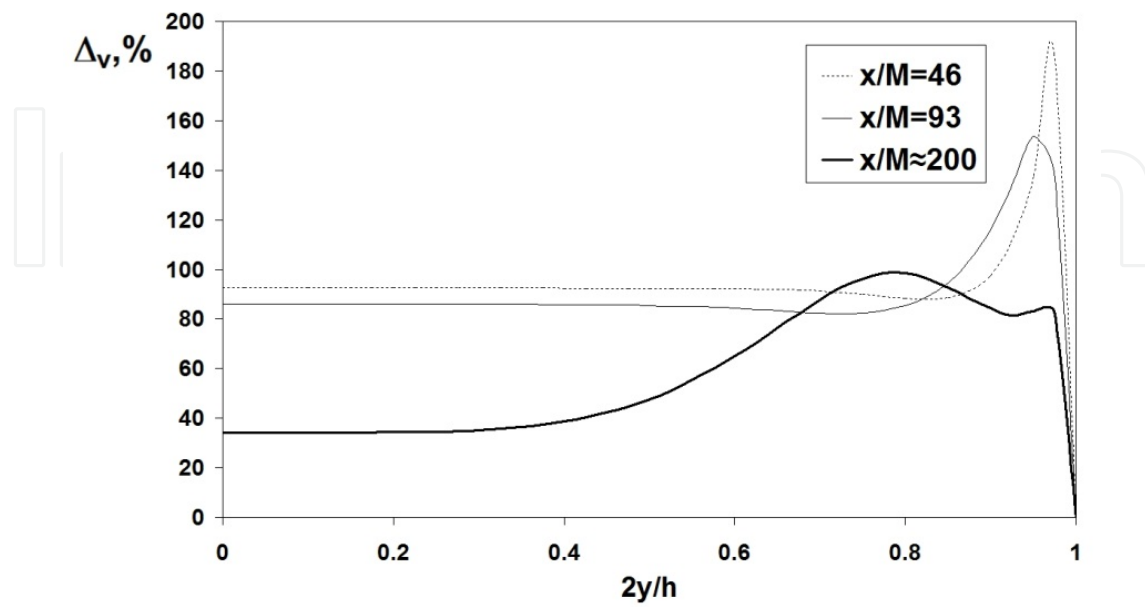
Figure 7. Effect of particles on the modification of the *y*-normal component of the Reynolds stress: *M*=4.8 mm, *z*=0.

Figure 8. Effect of particles on the modification of the *z*-normal component of the Reynolds stress: *M*=4.8 mm, *z*=0.
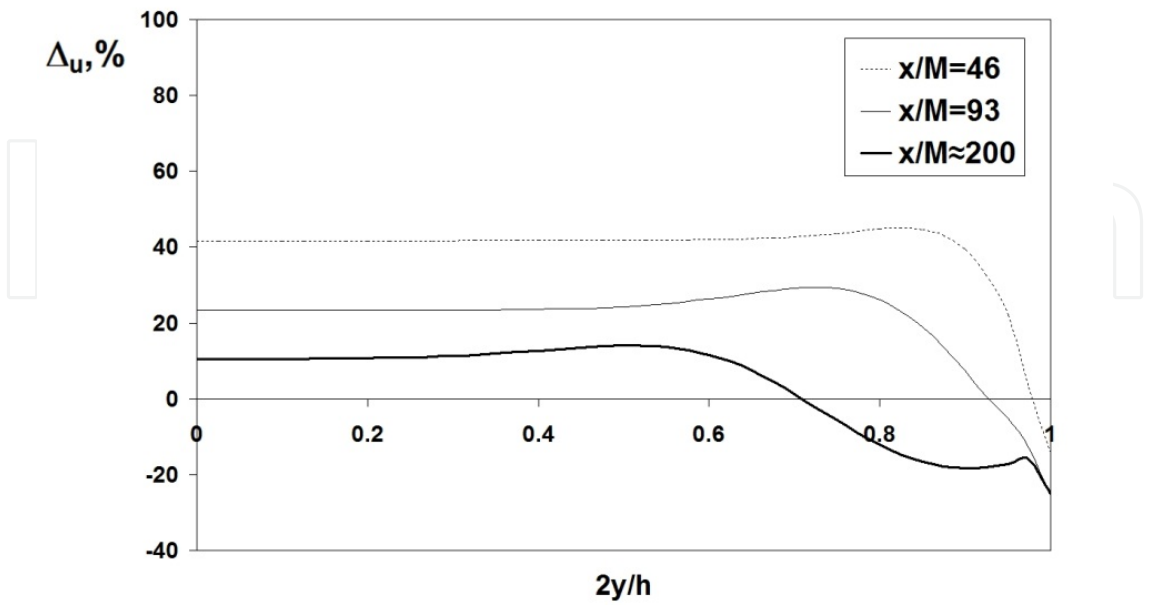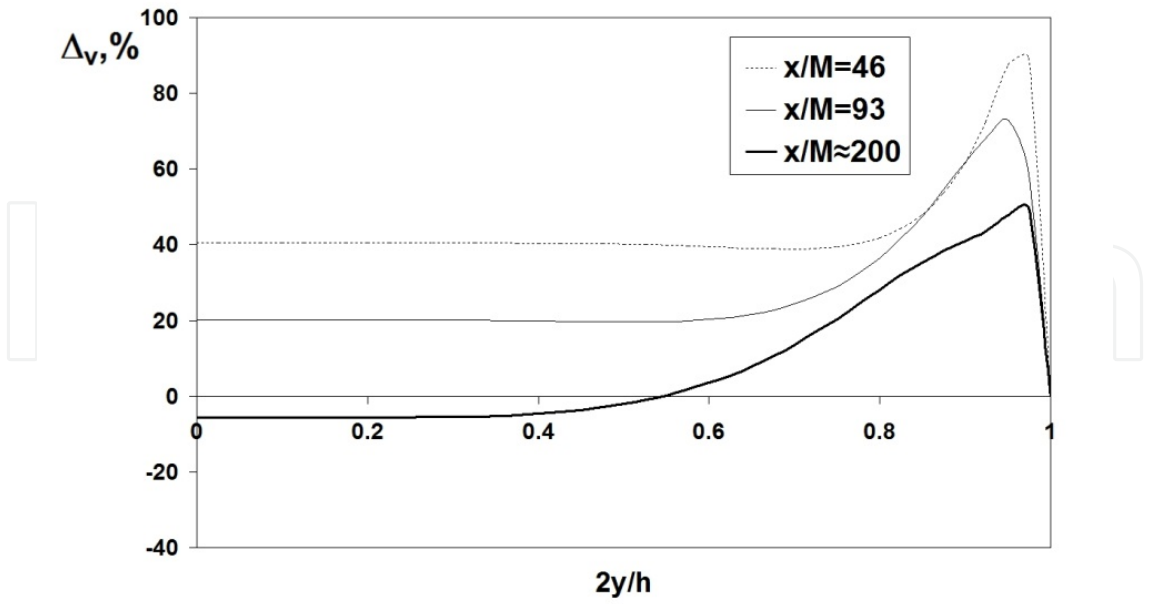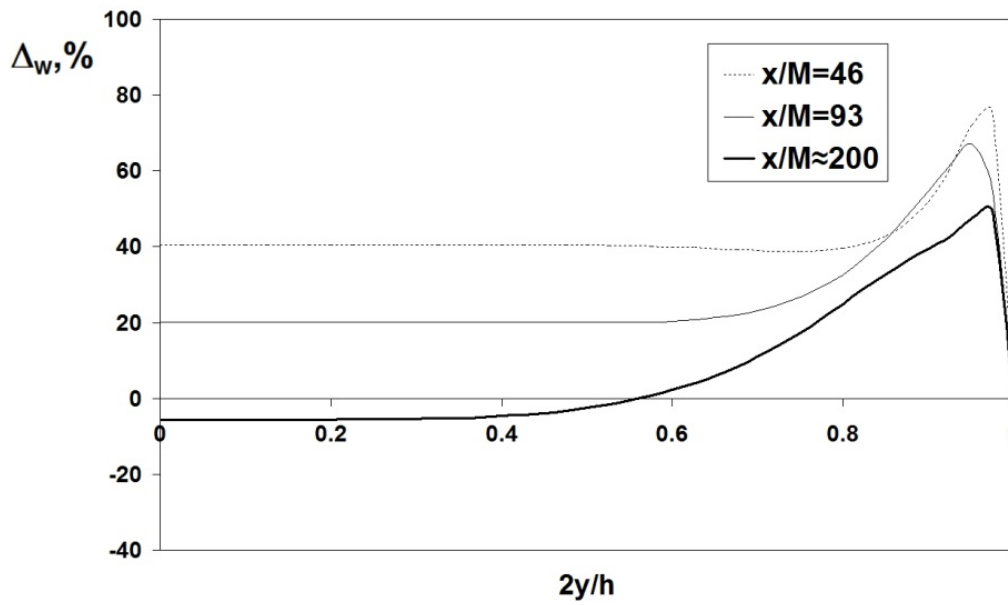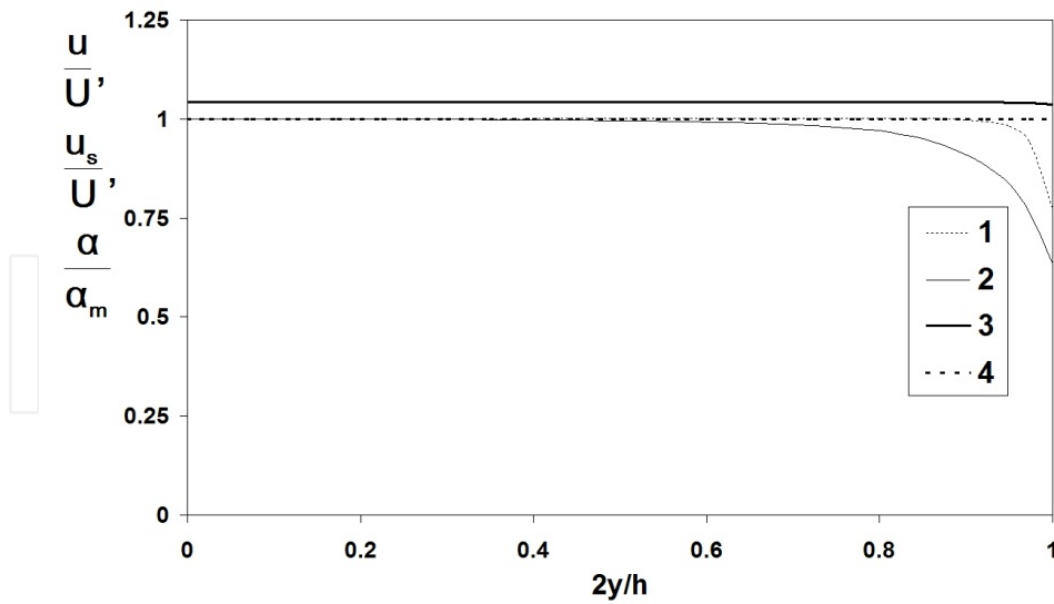
Figure 9. Effect of particles on the modification of the *x*-normal component of the Reynolds stress: *M*=10 mm, *z*=0.
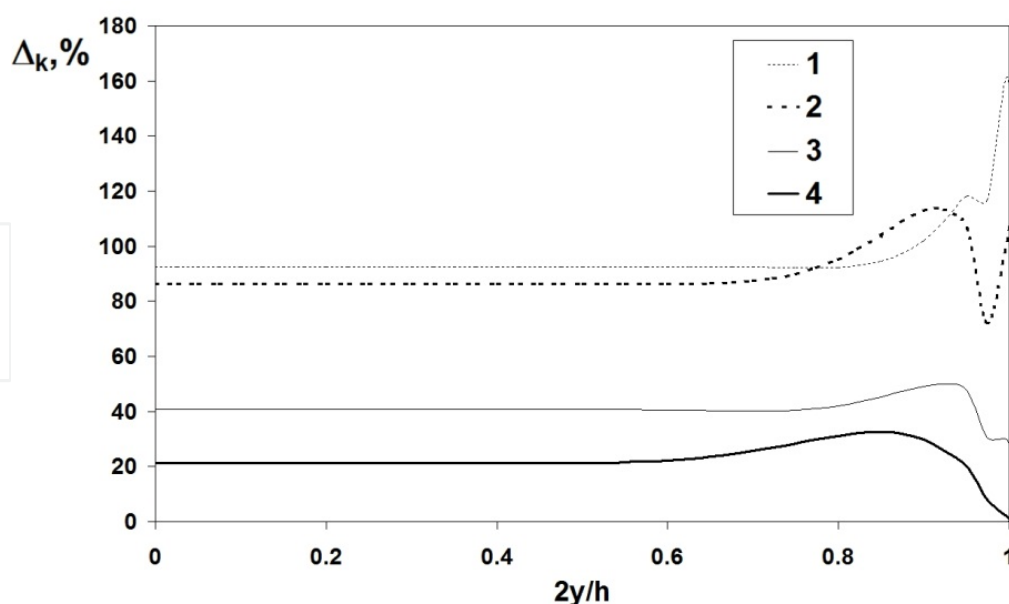

Figure 10. Effect of particles on the modification of the *y*-normal component of the Reynolds stress: *M*=10 mm, *z*=0.

Figure 11. Effect of particles on the modification of the *z*-normal component of the Reynolds stress: *M*=10 mm, *z*=0.

Figure 12. The cross-section distributions of the axial gas and particles velocities and particles mass concentration for the grid *M*=4.8 mm: 1 –*u* / *U* for *x* / *M* =46; 2 –*u* / *U* , 3 –u_s / *U* and 4 –*a* / a_m for *x* / *M* ≈ 200. Here a_m is the value of the mass concentration occurring at the flow axis.

Figure 13. Effect of particles on the modification of the turbulence kinetic energy: 1 –$M = 4.8$mm,$x / M = 46$; 2 – $M = 4.8$mm,$x / M = 93$; 3 –$M = 10$mm,$x / M = 46$; 4 –$M = 10$mm,$x / M = 93$.

The analysis of Figure 13 shows that the increase of the grid mesh size results in the weaker contribution of particles to the turbulence enhancement and dissipation of the kinetic energy taking place over the cross-section for the initial period of the turbulence decay. This can be explained by the higher rate of the particles involvement into the turbulent motion due to the longer residence time that comes from the larger size of the eddies.

4. Conclusions

The RSTM model has been elaborated for the horizontal and vertical turbulent particulate flows in the channels of rectangular and square cross-sections with the smooth and rough walls.

The present RSTM model has been validated for the unladen channel gas flow with the rough wall. It satisfactorily described the experimental data on the averaged gas axial velocity and three components of the turbulence energy.

Further, the present model was applied to simulate the vertical grid-generated turbulent particulate channel flow. It considered both the enhancement and attenuation of turbulence by means of the additional terms of the transport equations of the normal Reynolds stress components. The model allowed to carry out the calculations covering the long distance of the channel length without using algebraic assumptions for various components of the Reynolds stress. The numerical results showed the effects of the particles and the mesh size of the turbulence generating grids on the turbulence modification that had been observed in

experiments. It was obtained that the character of modification of all three normal components of the Reynolds stress taken place at the initial period of the turbulence decay are uniform almost all over the channel cross-sections. The increase of the grid mesh size slows down the rate of the turbulence enhancement which is caused by particles.

Acknowledgements

Author details

Alexander Kartushinsky[1*], Ylo Rudi[1], Medhat Hussainov[1], Igor Shcheglov[1], Sergei Tisler[1], Igor Krupenski[1] and David Stock[2]

*Address all correspondence to: aleksander.kartusinski@ttu.ee

1 Research Laboratory of Multiphase Media Physics, Faculty of Science, Tallinn University of Technology, Tallinn, Estonia

2 School of Mechanical and Materials Engineering, Washington State University, Pullman, Washington, USA

References

[1] Elghobashi S.E., Abou-Arab T.W. A Two-Equation Turbulence Model for Two-Phase Flows. Physics of Fluids 1983; 26(4) 931-938.

[2] Pourahmadi F., Humphrey J.A.C. Modeling Solid-Fluid Turbulent Flows with Application to Predicting Erosive Wear. International Journal of Physicochemical Hydrodynamics 1983; 4(3) 191-219.

[3] Rizk M.A., Elghobashi S.E. A Two-Equation Turbulence Model for Dispersed Dilute Confined Two-Phase Flows. International Journal of Multiphase Flow 1989; 15(1) 119-133.

[4] Simonin O. Eulerian formulation for particle dispersion in turbulent two-phase flows. In: Sommerfeld M, Wennerberg D. (eds.) Proceedings of the 5th Workshop on Two-Phase Flow Predictions, 19-22 March 1990, Erlangen, Germany. Ju◉lich: Forschungszentrum Ju◉lich; 1990.

[5] Deutsch E., Simonin O. Large eddy simulation applied to the motion of particles in stationary homogeneous fluid turbulence. In: Michaelides EE, Fukano T, Serizawa A. (eds.) Proceedings of the 1st ASME/JSME Fluids Engineering Conference, 23-27 June 1991, Portland, USA. New York: American Society of Mechanical Engineers, Series FED; 1991.

[6] Shraiber AA, Yatsenko VP, Gavin LB, Naumov VA. Turbulent Flows in Gas Suspensions. New York: Hemisphere Pub. Corp.; 1990.

[7] Crowe C.T., Gillandt I. Turbulence modulation of fluid-particle flows – a basic approach. In: Proceedings of the 3rd International Conference on Multiphase Flow, 8-12 June 1998, Lyon, France. CD-ROM.

[8] Crowe C. T. On Models for Turbulence Modulation in Fluid-Particle Flows. International Journal of Multiphase Flow 2000; 26(5) 719-727.

[9] Reeks M.W. On a Kinetic Equation for the Transport of Particles in Turbulent flows. Physics of Fluids A: Fluid Dynamics 1991; 3(3) 446-456.

[10] Reeks M.W. On the Continuum Equations for Dispersed Particles in Nonuniform Flows. Physics of Fluids A: Fluid Dynamics 1992; 4(6) 1290-1303.

[11] Zaichik L.I., Vinberg A.A. Modeling of particle dynamics and heat transfer in turbulent flows using equations for first and second moments of velocity and temperature fluctuations. In: Durst F, Friedrich R, Launder BE, Schmidt FW, Schumann U, Whitelaw, JH. (eds.) Proceedings of the 8th International Symposium on Turbulent Shear Flows, 9-11 September 1991, Munich, Germany. Berlin: Springer-Verlag; 1993.

[12] Zaichik L.I., Fede P., Simonin O., Alipchenkov V.M. Comparison of two statistical approaches for modeling collision in bidisperse mixture of particles settling in homogeneous turbulent flows. In: Sommerfeld M. (ed.) Proceedings of the 6th International Conference on Multiphase Flow, 9-13 July 2007, Leipzig, Germany. CD-ROM.

[13] Kartushinsky A.I., Michaelides E.E., Zaichik L.I. Comparison of the RANS and PDF Methods for Air-Particle Flows. International Journal of Multiphase Flow 2009; 35(10) 914-923.

[14] Gerolymos G.A., Vallet I. Contribution to single-point-closure Reynolds-stress modeling of inhomogeneous flow. In: Proceedings of the 4th ASME/JSME Joint Fluids Summer Engineering Conference FEDSM2003, 6-10 July 2003, Honolulu, Hawaii, USA. CD-ROM.

[15] Taulbee D.B., Mashayek F., Barré C. Simulation and Reynolds Stress Modeling of Particle-Laden Turbulent Shear Flows. International Journal of Heat and Fluid Flow 1999; 20(4) 368-373.

[16] Mukin R.V., Zaichik L.I. Nonlinear Algebraic Reynolds Stress Model for Two-Phase Turbulent Flows Laden with Small Heavy Particles. International Journal of Heat and Fluid Flow 2012; 33(1) 81-91.

[17] Launder B.E., Reece G.J., Rodi W. Progress in the Development of a Reynolds-Stress Turbulence Closure. Journal of Fluid Mechanics 1975; 68(3) 537-566.

[18] Pope SB. Turbulent Flows. Cambridge – New York: Cambridge University Press; 2008.

[19] Schiller L., Naumann A. Über die grundlegenden Berechnungen bei der Schwerkraftaufbereitung. Zeitschrift des Vereines deutscher Ingenieure 1933; 77 318-320.

[20] Zaichik L.I., Alipchenkov V.M. Statistical Models for Predicting Particle Dispersion and Preferential Concentration in Turbulent Flows. International Journal of Heat and Fluid Flow 2005; 26(3) 416-430.

[21] Perić M., Scheuerer G. CAST – A Finite Volume Method for Predicting Two-Dimensional Flow and Heat Transfer Phenomena. GRS - Technische Notiz SRR–89–01. 1989

[22] Hanjalic K., Launder B.E. Fully Developed Asymmetric Flow in a Plane Channel. Journal of Fluid Mechanics 1972; 51(2) 301-335.

[23] Hussainov M., Kartushinsky A., Rudi Y., Shcheglov I., Tisler, S. Experimental Study of the Effect of Velocity Slip and Mass Loading on the Modification of Grid-Generated Turbulence in Gas-Solid Particles Flows. Proceedings of the Estonian Academy of Sciences. Engineering 2005; 11(2) 169-180.

[24] Hinze JO. Turbulence. New York: McGraw-Hill; 1975.

[25] Kartushinsky A.I., Michaelides E.E., Hussainov M., Rudi Y. Effects of the Variation of Mass Loading and Particle Density in Gas-Solid Particle Flow in Pipes. Powder Technology 2009; 193(2) 176-181.